Transient Pellet-Cladding Interaction of LMFBR Fuel Rods – Computer Code ISUNE-5

B.M. Ma
Department of Nuclear Engineering, Iowa State University, 261 Sweeney Hall, Ames, Iowa 50010, U.S.A.

Summary

The transient fuel pellet-cladding interaction (PCI) of liquid-metal fast breeder reactor (LMFBR) fuel elements or rods is analyzed based on experimental results. The heat generation, ramp linear power rating, fuel restructuring, temperature distribution, bonding gap conductance, irradiation swelling, irradiation creep, fuel burnup, fission gas release, fuel pellet and cladding cracking, crack healing, radiation and oxidation corrosion, stress fatigue cracking, stress corrosion cracking, fuel performance, and reactor safety are taken into consideration. To improve the mixed $(U, Pu)O_2$ or (U, Pu)C fuel performance and reactor safety, it is desired to: (a) increase the strength and ductility of structural material; (b) provide adequate gap distance and plenum space; (c) keep ramp-power increase rate slow, and (d) reduce the intensity and frequency of transient PCI in order to minimize SFC and SCC.

1. Introduction

The transient fuel pellet-cladding interaction (PCI) can have a significant effect on fuel performance and burnup, fuel-element integrity, reactor safety, and core operating lifetime of a liquid-metal fast breeder reactor (LMFBR). The combination of thermal, nuclear, irradiation, chemical and mechanical factors with the fuel, bonding and structural (or cladding) materials induces the PCI; it can result in thermal expansion, thermal shock, thermal fatigue, thermal-cycling growth, fuel densification, irradiation swelling, irradiation creep, stress fatigue cracking (SFC), and stress corrosion cracking (SCC) at the interface of the pellet and cladding. A large number of experimental measurements, both in and out of reactor, and post-irradiation and post-failure examinations supported these results [1].

During reactor operation, the most important factors in these combined effects are (1) fuel pellet-cladding gap opening and closure, (2) irradiation damage in the fuel elements or rods, (3) corrosion, reducing the strength and integrity of the fuel element, and (4) fuel cracking, fission gas release, and induced stresses and strains to initiate SFC and/or SCC. These factors can cause central fuel meltdown and/or cladding breach and affect reactor safety.

In previous papers [2,3] the thermal, radiation and mechanical analyses for unsteady-state fuel restructuring of cylindrical oxide fuel elements in a LMFBR and Computer Code ISUNE-1 and the fuel pellet-cladding interaction of LWR fuel elements at unsteady state were introduced. The main objectives of this paper are:

1. To analyze the principal cause and effect of transient PCI on gap conductance, gap opening, gap closure, and gap partial opening and partial closure.

2. To extend the basic crack theory proposed for the fuel-cladding cracking and compare the predicted results with experimental data observed.

3. To improve the fuel performance, fuel rod reliability, and reactor safety at high neutron fluence, irradiation temperature, and fuel burnup.

2. Heat Generation Rate, Heat Transfer, and Temperature Distribution in Cladding

Let $\Sigma_f(E)$ = the macroscopic fission cross section, $\phi(r,E)$ = the average energy-radial-dependent fast neutron flux, and E = the average nuclear energy liberated per fission. Then the volumetric heat generation rate q_V is expressed as

$$q_V = E \int \Sigma_f(E)\phi(r,E)dE \cong E\bar{\Sigma}_f\phi(r) \tag{1}$$

When the design or operating coolant temperature, T_c, is given, the outer and inner clad surface temperatures, T_o and T_i, and the temperature distribution, T(r), in the cladding from heat generation of the fuel can be found from the basic heat transfer equations

$$T_o = T_c + \frac{q}{2\pi r_o h} \tag{2}$$

$$T(r) = T_o + \frac{q}{2\pi k_c} \ln\left(\frac{r_o}{r}\right) \tag{3}$$

$$T_i = T_o + \frac{q}{2\pi k_c} \ln\left(\frac{r_o}{r_i}\right) \tag{4}$$

where q is the linear power rating of fuel element, k_c is thermal conductivity of the cladding material, and h is heat transfer coefficient between coolant and cladding. The heat transfer coefficient is determined from the Nusselt number N_{Nu} for the sodium coolant [4,5]:

$$N_{Nu} = hD_e/K = 6.66 + 3.126(s/d) + 1.184(s/d)^2 + 0.0155(\psi/N_{Pe})^{0.86} \tag{5}$$

$$\psi \equiv 1 - 0.942(s/d)^2/N_{Pr}(N_{Re}/10^3)^{1.281} \tag{6}$$

where N_{Pe} is the Peclet number, N_{Pr} is the Prandtl number, N_{Re} is the Reynolds number, D_e is the equivalent diameter of the coolant channel, K is the thermal conductivity of the Na coolant, and s/d is the ratio of fuel lattice pitch to rod diameter.

If ε_{θ_i} and ε_{thc} are the tangential and thermal (expansion) strains at the inner clad radius r_i; ε_{θ_s}, ε_{thf} and ε_I are tangential, thermal (expansion) and irradiation swelling strains at the outer fuel radius r_s; and K_{gap} is the thermal conductivity of the bonding gap to be determined, the relationship between temperature T_s at the outer fuel surface and temperature T_i at the inner clad surface is given by [6] (see Eq. (4))

$$T_s = T_i + \frac{q}{2\pi K_{gap}} \ln\left[r_i(1 + \varepsilon_{\theta_i} + \varepsilon_{thc})/r_s(1 + \varepsilon_{\theta_s} + \varepsilon_{thf} + \varepsilon_I)\right] \tag{7}$$

Therefore, the heat generated from the fuel passes through the bonding gap and the cladding of the fuel elements or rod to the coolant by means of heat transfer.

3. Linear Power Rating and Temperature Distribution in Fuel

Fuel restructuring (or grain growth) and redistribution occur in the ceramic fuel after a sufficient period of neutron irradiation. In the fuel restructuring process, four distinct regions (or zones) are formed: (1) central void, (2) columnar grain region, (3) equiaxed grain region, and (4) sintered or unaffected grain region in the fuel, as shown in Fig. 1.

The distribution of fast neturon flux ϕ in the fuel is essentially uniform. For a given linear power rating q, the volumetric heat generation rate q_v per unit length in the unaffected grain region, equiaxed grain region, and columnar grain region is expressed as

$$q_{v3} = q/\pi r_s^2, \quad q_{v2} = q_{v3}\ \rho_2/\rho_3, \quad q_{v1} = q_{v3}\ \rho_1/\rho_3 \tag{8}$$

where ρ_1, ρ_2, and ρ_3 are the actual smeared densities (fractions of theoretical density, TD) of the mixed fuel $(U,Pu)O_2$ in the three regions (Fig. 1).

In the transient reactor operation during power up or power down, the linear power rating varies with time and slope m as ramp functions from a base linear power rating q_o:

$$q = q_o\ (1 + mt) \quad \text{(power up)}; \qquad q = q_o\ (1 - mt) \quad \text{(power down)} \tag{9}$$

The thermal conductivity K or K_f of the mixed oxide fuel depends on the fuel temperature T and fuel density ρ for a prescribed fuel preparation and sintering process [1]:

$$K = K_f(T,\rho) = C_1 + [T(C_2 - C_3\rho)]^{-1} \tag{10}$$

where C_1, C_2 and C_3 are constants [2].

To determine the temperature distribution in the fuel, the heat conduction per unit volume of the unaffected grain region is first considered. At any given time t, by angular and axial symmetry and in the equilibrium state of heat generation, the heat conduction is

$$\frac{d^2T}{dr^2} + \frac{1}{r}\frac{dT}{dr} = -\frac{q_v}{K} = -\frac{q_{v3}}{K} \tag{11}$$

Substituting Eqs. (8) and (10) into Eq. (11) and integrating with appropriate limits, temperature distributions in the unaffected grain, equiaxed grain, and columnar grain regions have been derived [2,3].

From the balance of power output before and after formation of the four regions in fuel restructuring, a relation to determine the central void radius, or r_v/r_1 is

$$r_v/r_1 = [(r_2/r_1)^2\ (q_{v2} - q_{v3})/q_{v1} + (q_{v1} - q_{v3})/q_{v1}]^{1/2} \tag{12}$$

Therefore, from the derived temperature distribution equations and Eq. (12), the values of r_2/r_s, T_2/T_s, r_1/r_2, T_1/T_2, T_v/T_i, and r_v/r_1 can be found.

With a sufficiently long, high-temperature operation during fuel restructuring, columnar grain growth is developed by the formation and movement of porosity-fabricated pores of fission gases out of this region. The pores move up with the thermal gradients. Migration up to the central region results in central void and columnar grain region. The fuel density ρ_3 is usually 99-100% TD. The velocity v of a migrating pore has been given in reference [2].

Since the temperature distribution in fuel is parabolic or exponential [2], the average thermal gradient $(\partial T/\partial r)_{av}$ occurs at $r_s/3$, and this threshold temperature for columnar grain and concomitant central void formation as a function of time t is given by

$$r_s/3t = [C_4 \exp(-C_5/T)T^{3/2}]\ (\partial T/\partial r)_{av} \tag{13}$$

where C_4 and C_5 are constants. For known values of r_s, t and $(\partial T/\partial r)_{av}$, the threshold central temperature T_c or T_v can be obtained from Eq. (13).

The equiaxed grain growth related to the initial grain size D_o before irradiation and grain size D after irradiation through time t is given by

$$D^3 - D_a^3 = k_o t \exp(-Q/RT) \tag{14}$$

where k_o is a constant, Q is the activation energy, R is the universal gas constant, and T is the temperature during the process of equiaxed grain growth. Figure 2 shows typical variations of calculated and measured centerline temperature with linear power rating of the oxide fuel element.

4. Gap Conductance and Pellet-Cladding Interaction (PCI)

With either helium or sodium as the bonding material between the fuel pellet and cladding of LMFBR fuel elements, the main functions of the bonding gap have been given in (3).

Originally, the bonding gap is open. Causes of gap closure include thermal expansion, irradiation growth, irradiation swelling, irradiation creep, and radial-circumferential dislocations of fuel cracking. Gap opening, closure, and reopening can affect gap conductance (or heat transfer coefficient) h_{gap}. As predicted theoretically and observed experimentally, partial or complete gap closure occurs when new fuel elements are in operation [7]. Irradiation-induced fuel densification, crack healing, and/or power down could cause the gap to reopen [7].

4.1. Gap Opening and Gap Conductance

Gap conductance h_{gap} consists of gas conductance h_{gas}, radiant heat conductance h_r, and gas surface constriction conductance h_s. In the case of gap opening during operation, the gap conductance is expressed as

$$h_{gap} = h_{gas} + h_r, \qquad h_s = 0 \tag{15}$$

When the gap length, L_g, between the fuel pellet and cladding is sufficiently large,

$$L_g = r_i(1 + e_{\theta_i} + \varepsilon_{thc}) - r_s(1 + e_{\theta_s} + \varepsilon_{thf} + \varepsilon_I) \geq a_1(\delta_1 + \delta_2) \tag{16}$$

The gas conductance is represented by

$$h_{gas} = K_{gas}/[(L_g + \xi_f + \xi_c) + a_1(\delta_f + \delta_c)] \tag{17}$$

where K_{gas} is the thermal conductivity of the fission, volatile and bonding gases (or vapors), a_1 is constant about 1.10-1.25, δ_f and δ_c are arithmetic mean roughness heights of the fuel and clad surfaces, and ξ_f and ξ_c are the temperature jump distances of the fuel and clad.

The radiant heat conductance h_r is derived from the relations of the balance of radiant heat flux, $q_{rad/A}$, and the Stefan-Boltzmann law [7]

$$h_r = \sigma_{SB}[e_f^{-1} + e_c^{-1} - 1]^{-1} (T_s + T_i) (T_3^2 + T_i^2) \tag{18}$$

Introducing Eqs. (17) and (18) into Eq. (15), the gas conductance for the gap opening is

$$(h_{gap})_o = \frac{K_{gas}}{L_g + \xi_f + \xi_c + a_1(\delta_f + \delta_c)} + \sigma_{SB}\left[e_f^{-1} + e_c^{-1} - 1\right]^{-1} (T_s + T_i) (T_s^2 + T_i^2) \tag{19}$$

where σ_{SB} is the Stefan-Boltzmann constant, e_f and e_c are emissivities of the outer fuel and

inner clad surfaces, and T_s and T_i are the fuel and clad surface temperatures.

4.2. Complete Gap Closure

In the case of complete gap closure, L_g vanishes and the gap conductance is

$$h_{gap} = h_{gas} + h_r + h_s \tag{20}$$

If $K_m = 2k_f K_c/(K_f + K_c)$, the harmonic mean of fuel and clad thermal conductivities, P_m is the interfacial contact pressure between fuel and clad surfaces, a is the radius of interface-contact spot due to P_m, H is effective hardness of the clad (e.g., for stainless steel 316, $H = 1.5(10^4)Kg/cm^2$), then the gap conductance for the complete gap closure is given by

$$(h_{gap})_c = \frac{K_{gas}}{\xi_f + \xi_c + a_1(\delta_f + \delta_c)} + \sigma_{SB}\left[e_f^{-1} + e_f^{-1} - 1\right]^{-1}(T_s + T_i)(T_s^2 + T_i^2) + \frac{K_m P_m}{aH} \tag{21}$$

For a very thin gap, the mean temperature of the gases contained in the gap is taken as

$$T_g = (T_s + T_i)/2 = (T_o + T_i)/2 \tag{22}$$

The thermal conductivity of the gaseous gap K_{gap} can then be obtained approximately by adding the gas thermal conductivity K_{gas} and the radiant thermal conductivity K_r:

$$K_{gap} = K_{gas} + K_r = K_{gas} + 4L_g \sigma_{SB}\left[e_f^{-1} + e_c^{-1} - 1\right]^{-1} T_g^3 \tag{23}$$

4.3. Gap Partially Open and Partially Closed: "Bambooing" (or Ridging)

When the gap is partially open and partially closed due to "bambooing" along the axial direction of the fuel element, a mean gap conductance is approximated from Eqs. (19) and (21):

$$h_{gap} = [(h_{gap})_o + (h_{gap})_c]/2 \tag{24}$$

The cause for partial gap opening and partial gap closure is the "bambooing" of the ceramic fuel element: lateral expansion outward at each end contrasts to the lateral shrinkage near the midsection of each fuel pellet. This is attributed to the combined effects of fuel densification, isotopic shrinkage, restricted thermal expansion, irradiation swelling, and induced stresses and strains in different proportions at different locations on the fuel pellet and, consequently, cladding.

Verification of the predicted (by the computer code) and measured gap conductance reported for UO_2 and $(U,Pu)O_2$ fuel pellets with He bonding is given in Fig. 3.

5. Irradiation Swelling in Fuel and Structural Materials

Apart from thermal-cycling and irradiation growth, the most important irradiation effects on nuclear fuel and structural or cladding materials are swelling and creep, which limit the performance of fuel elements or rods and affect reactor safety and economics.

Irradiation swelling in the ceramic fuel is composed of (1) fission product solid solution swelling and (2) inert fission gas swelling (major part). The total change in volume, $\Delta V/V$, due to irradiation swelling has been derived [2]. For irradiation swelling in structural (or cladding) material from experimental data of cold-worked stainless steel (Types 304, 316) as well as high-temperature nickel alloys (Inconel-600, Incoloy-825), the empirical equations for change in volume obtained from transmission electron microscopy (TEM) and macroscopic dimension measurement (MDM) plotted in Fig. 4 are in good agreement.

6. Irradiation Creep in Fuel and Structural Materials

On the basis of analytical results and experimental data, it was postulated that the irradiation creep strain ε and creep strain rate $\dot{\varepsilon}$ of the ceramic fuel are represented by the power function creep law [3]. In the same manner, the irradiation creep strain ε and creep strain rate $\dot{\varepsilon}$ at creep stress σ, neutron flux ϕ, irradiation time t and irradiation temperature T of the structural material were postulated [3].

7. Fuel Burnup and Fission Gas Release

Fuel burnup, BU, is equal to fission rate $\dot{F}$ multiplied by time t:

$$BU = \dot{F}t \tag{25}$$

Fission gas release is mainly a function of fuel irradiation temperature and burnup, as is irradiation swelling in fuel. Figure 5 shows the variation of irradiation swelling and fission gas release measured with fuel temperature and burnup of $(U,Pu)O_2$.

8. Fuel Pellet and Cladding Cracking and Crack Healing

Crack nucleation and crack propagation are caused mainly by thermal shock, thermal-cycling fatigue, nonuniform thermal expansion, and stress corrosion effect. It was postulated that shearing stress (microstructural, intergranular, and macroscopic stress) nucleates cracks and that principal stress propagates and extends cracks along the plane normal to that stress. Experimental results verify the theoretical prediction [8], as well as SFC and SCC.

Fission gases containing I, Cd, Te and their compounds such as CsI, CdI_2, Cs_2Te released from the radial cracks of the fuel pellets can readily attack the inner surface of the clad through the PCI, opposite to fuel pellet cracks [6].

Crack healing is related to annealing grain growth. The recovery in mechanical strength and ductility or rate of crack healing depends on the irradiation-annealing temperature T, time t, and stress σ. It is postulated that the rate of crack healing, $\partial c/\partial t$, is a function of a second-order (inelastic) property of crack length c and irradiation temperature T:

$$\partial c/\partial t = gc^2 \exp(-Q/RT) \equiv g_T c^2 \tag{26}$$

where g is a constant, and $g_T = g \exp(-Q/RT)$ as defined. The relation for crack length c and fracture strength σ of a cylindrical fuel pellet (or clad) is expressed as

$$\sigma = (E\eta/\pi c)^{1/2} \tag{27}$$

where E is the elastic modulus and η is specific energy per unit area of the material. Integrating Eq. (26) from $t = 0$ for $c = c_o$ (the maximum crack length before healing) to any time t for any crack length c during crack healing, the crack ratio is

$$c/c_o = (1 + c_o g_T t)^{-1} \tag{28}$$

At the end of complete healing time, t_f, when the original strength σ_f (or elastic limit) is recovered, by eliminating c/c_o the stress ratio is

$$\sigma_f/\sigma_o = (1 + E\eta g_T t/\pi\sigma_o^2)^{1/2} \tag{29}$$

Hence, the healing time required to recover the original strength of the material is

$$t_f = \pi(\sigma_f^2 - \sigma_o^2)/E\eta g_T \qquad \text{for } \sigma_f > \sigma_o \tag{30}$$

9. Sodium Corrosion of Structural Material

The effect of radiation and oxidation corrosion of high-temperature sodium coolant on structural materials such as stainless steel 304 or 316 in a LMFBR is to influence their strength, ductility and surface cracking [1]. The corrosion rate of liquid sodium depends mainly on impurities (O, C, N,..., especially oxygen content), clad temperature, coolant flow velocity, and exposure time. Theoretically, the corrosion rate follows a parabolic law at a given temperature [1]. Figure 6 shows variation of corrosion rate with clad surface temperature of the structural materials [9,10].

10. Introduction to Stress-Strain Analysis and Computer Code

Mechanical analyses for the LMFBR and LWR fuel elements or rods have been carried out on the basis of the basic assumptions and experimental results [2,6]. From the stress and strain equations derived and the important variables as the functions of radial space and irradiation time of the fuel element selected, schematic flow charts of Computer Code ISUNE-5 are programmed, similar to the general flow chart and the stress-strain flow chart used in Computer Codes ISUNE-1 and ISUNE-4 [2,6]. With selected input data and material constants, these important variables for temperature distributions, fuel performance, gap conductance, irradiation swelling, sodium corrosion rate, etc. are computed (see Figs. 2, 4-6).

11. Conclusions

From the preceding analysis for transient fuel pellet-cladding interaction of LMFBR fuel element or rod with Computer Code ISUNE-5, the following main conclusions are drawn:

1. Temperature distribution, fuel cracking, and change in gap conductance vary with the radial space, irradiation time and linear power rating of the fuel element or rod.
2. At a ramp linear power rating, because of fuel restructuring the radii of central void, columnar grain, equiaxed grain and unaffected grain regions near the midplane of the fuel element change appreciably to affect the fuel cracking and PCI.
3. The basic crack theory was postulated and verified by experimental observation and postirradiation examination for SFC and/or SCC during PCI. The fission products I, Cd, Te and their compounds CsI, CdI_2, Cs_2Te, etc. can attack the inner clad surface for nucleation of SCC. The corrosion rate increases with oxygen content, clad surface temperature and exposure time in high-temperature sodium coolant.
4. To improve fuel performance and reactor safety, it is necessary to (a) increase the mechanical strength and ductility of the structural material, (b) provide adequate bonding gap distance and plenum space for fission gas accommodation, (c) keep the ramp power increase rate slow, and (d) reduce the intensity and frequency of transient PCI of LMFBR fuel element or rod.

References

1. MA, B. M., Nuclear Reactor Materials and Applications, Von Nostrand Reinhold Co. 1982.
2. CHENG, C. K. and MA, B. M., "Thermal, Radiaton and Mechanical Analysis for Unsteady State Fuel Reprocessing of Cylindrical Oxide Elements in Fast Reactor," Nucl. Sci. Eng., 48, 139-158 (1972).
3. MA, B. M., "Pellet-Cladding Interaction of LMFBR Fuel Elements at Unsteady State," ASME J. Eng. Power, 103, 827 (1981).
4. DWYER, O. E., Liquid Metal Handbook, Sodium and Nak Supplements, U.S. AEC, 170.
5. DWYER, O. E., BARRY, H. C. and HLAVAC, P. J., Nuc. Eng. Des. 23, 273-295 (1972).
6. MA, B. M., "Transient Pellet-Cladding Interaction of LWR Fuel Rod-Computer Code ISUNE-4," Nuc. Eng. Des., 58, 303-338 (1980).
7. MA, B. M., "Irradiation Swelling, Creep and Thermal Stress Analysis of LWR Fuel Elements, Computer Code ISUNE-2," Nucl. Eng. Des., 34, 361-378 (1975).
8. MA, B. M., "Irradiation Swelling, Creep, Thermal-Shock and Thermal-Cycling Fatigue Analysis of Controlled Thermonuclear Reactor First Wall," Nucl. Eng. Des., 28, 1-30 (1974).
9. DARLEY, J. E. and WEEKS, J. R., Corrosion by Liquid Metals, Plenum Press, 1970.
10. WEBER, J. W., Proc. Int. Conf. Liq. Metal Tech. in Energy Production, 1, 378 (1975).

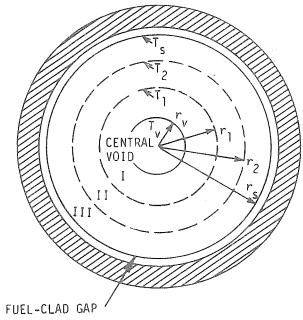

Fig. 1. Typical cross section of an irradiated oxide fuel element.

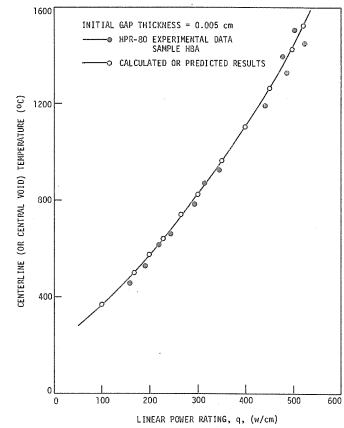

Fig. 2. Comparison of calculated and measured centerline temperature of the oxide fuel element.

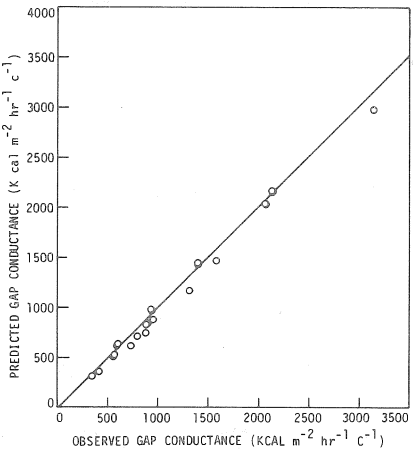

Fig. 3. Comparison of predicted and observed fuel pellet-cladding gap conductance.

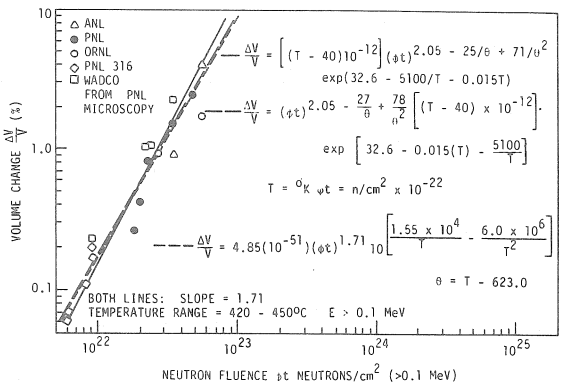

Fig. 4. Volume change varies with neutron fluence for 316 stain less steel.

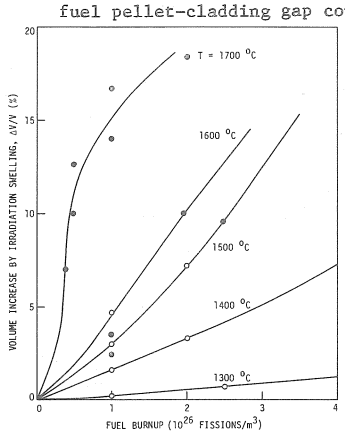

Fig. 5. Comparison of predicted and observed irradiation swelling varies with fuel burnup and irradiation temperature.

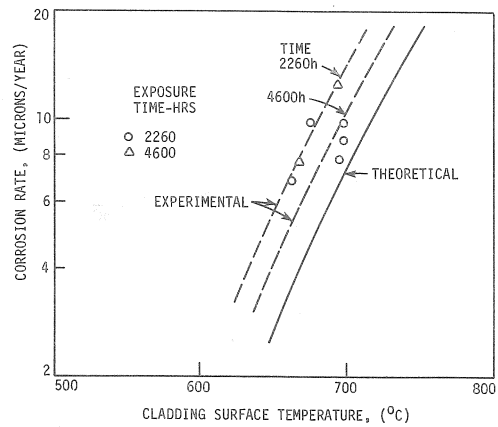

Fig. 6. Corrosion rate of 20% cold-worked stainless steel Type 316 varies with clad surface temperature.